AIP | Applied Physics Letters

Electronic structure of Ce3+ multicenters in yttrium aluminum garnets

H. Przybyliska, Chong-Geng Ma, M. G. Brik, A. Kamiska, P. Sybilski, A. Wittlin, M. Berkowski, Yu. Zorenko, V. Gorbenko, H. Wrzesinski, and A. Suchocki

Citation: Applied Physics Letters **102**, 241112 (2013); doi: 10.1063/1.4812190
View online: http://dx.doi.org/10.1063/1.4812190
View Table of Contents: http://scitation.aip.org/content/aip/journal/apl/102/24?ver=pdfcov
Published by the AIP Publishing

Electronic structure of Ce^{3+} multicenters in yttrium aluminum garnets

H. Przybylińska,[1] Chong-Geng Ma,[2] M. G. Brik,[2] A. Kamińska,[1] P. Sybilski,[1] A. Wittlin,[1,3] M. Berkowski,[1] Yu. Zorenko,[4] V. Gorbenko,[5] H. Wrzesinski,[4] and A. Suchocki[1,4]
[1]*Institute of Physics, Polish Academy of Sciences, Al. Lotników 32/46, 02-668 Warsaw, Poland*
[2]*Institute of Physics, University of Tartu, Riia 142, Tartu 51014, Estonia*
[3]*Cardinal Stefan Wyszyński University in Warsaw, ul. Dewajtis 5, 01-815 Warsaw, Poland*
[4]*Institute of Physics, Kazimierz Wielki University, Weyssenhoffa 11, 85-072 Bydgoszcz, Poland*
[5]*Department of Electronics of Ivan Franko National University of Lviv, Gen. Tarnavskyj Str., 107, 70017 Lviv, Ukraine*

(Received 2 April 2013; accepted 9 June 2013; published online 21 June 2013)

Low temperature, infrared, and visible-ultraviolet absorption spectra of yttrium aluminum garnet (YAG) bulk crystals and epitaxial layers doped with Ce are presented. In the region of intra-configurational 4*f*–4*f* transitions, the spectra of the bulk YAG crystals exhibit existence of at least two different Ce^{3+} related centers, a major one associated with Ce in regular positions substituting yttrium and also additional center, due to so called antisite positions in the garnet host, i.e., ions in the Al positions. Crystal field analysis based on exchange charge model exhibit excellent agreement with the experimental data for major Ce^{3+} center. © *2013 AIP Publishing LLC*.
[http://dx.doi.org/10.1063/1.4812190]

Cerium doped materials are the subject of numerous studies for solid state laser materials,[1,2] phosphors,[3–8] and scintillators.[9,10] Ce^{3+} has the simplest of the $4f^n$ ground state configurations ($n = 1$). In some garnets, Ce^{3+} ions form very efficient luminescence centers, originating from parity allowed inter-configurational $4f^0 5d^1 \rightarrow 4f^1 5d^0$ transitions; in the others, the luminescence is absent due to non-radiative energy transfer processes. $Y_3Al_5O_{12}$ (YAG) belongs to the first group of garnet crystals, while $Gd_3Ga_5O_{12}$ (GGG) and $Y_3Ga_5O_{12}$ (YGG) garnets represent the second one.[11]

Trivalent rare-earths dopants usually substitute yttrium dodecahedral sites in YAG structure. However, in Czochralski grown bulk crystals, so called antisites are also found, i.e., rare-earth ions replacing aluminum in sites with octahedral symmetry.[12] In addition, other types of rare-earth and transition metal centers occur often in garnets.[13] On the other hand, the YAG layers epitaxially grown from flux do not contain antisites of rare-earths.[14] This is due to the significantly lower (in the 950–990 °C range) growth temperature of the films in comparison with their bulk counterpart (2070 °C). It is of importance, since antisite defects influence optical properties of scintillator materials, having sometimes detrimental effects on their characteristics.

In spite of importance of YAG:Ce as a phosphor material, especially for white-lightning, there is a shortage of information on the details of the structure of Ce^{3+} multicenters in YAG. Certain evidences of the multisite structure of Ce ions are presented in recent paper by Feofilov *et al.*[15] Also a series of papers by Zorenko *et al.* have shown that Ce^{3+} antisites do not occur in flux grown thin layers of YAG:Ce. This conclusion is based on the analysis of the broad-band luminescence of self-trapped excitons in the ultraviolet (UV) spectral region.[16] In a recent paper, we demonstrated the existence of Ce^{3+}-related multisites in gadolinium gallium garnet bulk crystals.[17] In this paper, we present direct evidence of multisite incorporation of Ce^{3+} in YAG and identify the nature and energy structure of particular Ce-related centers.

The energy structure of Ce^{3+} ions with $4f^1$ configuration consists of a $^2F_{5/2}$ ground state and a $^2F_{7/2}$ excited state. Crystal field (CF) and spin-orbit interactions split these two states into three (levels #1–3) and four (levels #4–7) energy levels, respectively. Commonly, they are presented only as two levels separated by about 2200 cm^{-1}, as in the classic Dieke diagram.[18] Luminescence spectra of the d ↔ f transitions often support this picture since they can be deconvoluted into two semi-Gaussian bands separated by about 2000 cm^{-1}. The low-temperature, far-infrared absorption measurements show, however, that the splitting of the excited $^2F_{7/2}$ state in garnets is very large and extends up to about 4000 cm^{-1}. The theoretical crystal field analysis supports our experimental findings.[17]

The YAG:Ce bulk crystal used in our study was grown by the Czochralski method. The Ce content in the melt was set to 3 at. %. Due to the small value of the segregation coefficient, k ($k \ll 1$), the concentration of Ce in the crystal is expected to be around 0.5%. YAG:Ce single crystalline films were obtained at Institute of Physics of Kazimierz Wielki University in Bydgoszcz (Poland). The films were grown by liquid phase epitaxy (LPE) in a platinum crucible from the melt solution containing Y_2O_3, CeO_2, and Al_2O_3 oxides of 5N purity on both sides of (110) oriented YAG substrates.[19,20] For absorption studies, samples with total thickness between 60 and 130 μm were selected. The infrared absorption spectra were measured with a VERTEX 80v (Bruker) and a BOMEM DA3 Fourier-Transformed Infrared (FTIR) spectrometers, at a resolution of 1 cm^{-1}. Absorption in the visible spectral region was measured with CARY 5000 UV-VIS NIR spectrophotometer. For low temperature measurements, the samples were placed into an Oxford Instruments CF-102 continuous-flow cryostat equipped with KBr or quartz windows for infrared and UV-VIS measurements, respectively.

The transmission spectrum of the YAG:Ce (3%) bulk sample taken at 13 K in the region of the 4*f*–4*f* transitions is presented in Fig. 1. A spurious background, associated most

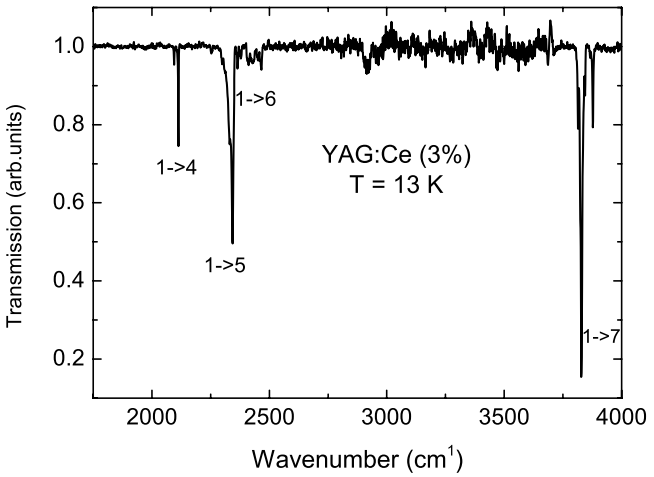

FIG. 1. Transmission spectrum of the bulk YAG:Ce (3%) sample taken at 13 K in the region of Ce^{3+} *4f-4f* transitions. Transitions designations are marked on the graph.

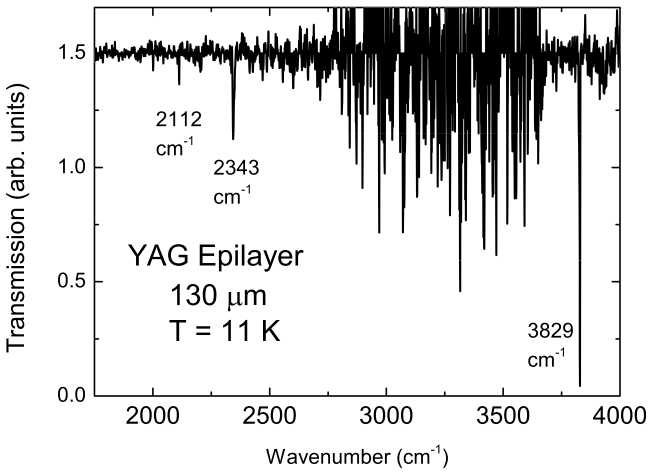

FIG. 3. Transmission spectrum of the YAG:Ce epitaxial layer sample taken at 11 K in the region of Ce^{3+} *4f-4f* transitions. Large noise-like signal between 2800 and 3600 cm^{-1} is associated with the very low reference signal in this spectral region.

probably with interferences induced by a thin film accidentally deposited on the sample surfaces during cooling, was subtracted from the spectra. The four groups of lines in Fig. 1 are attributed to optical transitions between the lowest-lying level (#1) of the ground $^2F_{5/2}$ state and four levels of the $^2F_{7/2}$ excited state of Ce^{3+}. Since each group consists of at least two lines, evidently more than one Ce^{3+} center contributes to the spectrum. The two lines associated with the 1 → 5 transition partly overlap.

Room-temperature absorption spectra of YGG: Ce^{3+}(3%) bulk crystal and epitaxial layer in the region of cerium 4*f*-4*f* intra-configurational transitions are presented in Fig. 2.

Two groups of lines associated with Ce^{3+}, in the region of 2000–2600 cm^{-1} and between 3200 and 3800 cm^{-1}, are visible in the spectra. The sharp lines around 2800 cm^{-1} are most probably related to OH vibrations. The strong absorption below 1800 cm^{-1} is due to Reststrahlen effects. The line peaked at 3538 cm^{-1} is a hot line due to transitions from the thermally populated level #2 of the $^2F_{5/2}$ ground state to level #7 of the $^2F_{7/2}$ excited state. The separation from the main line (originating from transitions between levels #1 and #7) locates level #2 of the ground state 290 cm^{-1} above level #1.

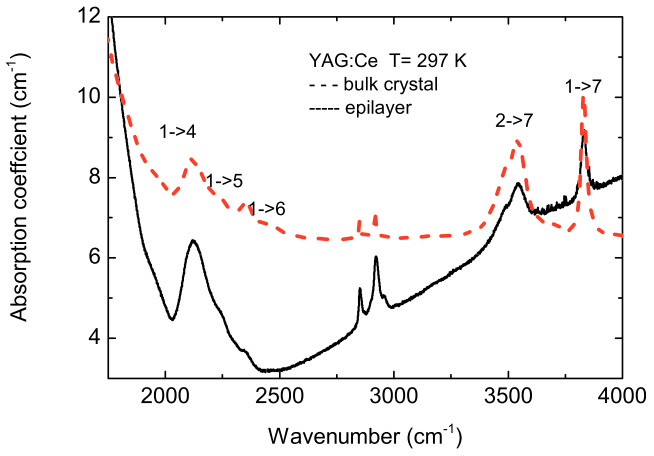

FIG. 2. Absorption spectra of Ce-doped YAG crystal and epitaxial layer at room temperature in the region of intra-configurational *4f* → *4f* transitions.

Room temperature spectra of the bulk crystal and epitaxially grown layer are very similar.

Low temperature transmission spectrum of YAG epitaxial layer is presented in Fig. 3

Only three lines associated with Ce^{3+} absorption are visible in the last spectrum, related to optical transitions between level #1 and levels #4, #5, and #7. This confirms that epitaxially grown layers hardly contain Ce^{3+} multicenters, in particular, the Ce antisites (Ce^{3+}_{Al}) are not observed here. Only lines associated with Ce^{3+} on Y sites (Ce^{3+}_{Y}) are visible, with exception of the low intensity line associated with transition between levels #1 and #6. In addition, the spectral lines at low temperatures are much sharper for epitaxially grown layer than for bulk crystal. For example, the full-width at half of maximum (FWHM) of the lines associated with transitions between levels #1 and #7 are equal to about 10 and 3.9 cm^{-1}, for the bulk crystal and the LPE layer, respectively. It testifies again that the number of Ce^{3+}-related multicenters in epitaxially grown layers is much lower than in bulk crystals and shows very good quality of these single crystalline films.

Low temperature absorption spectra of the YAG:Ce bulk crystal and epitaxial layer in the $4f^15d^0 \rightarrow 4f^05d^1$ transition region are shown in Fig. 4. The absorption bands peaked at 21 670 cm^{-1} and 29 710 cm^{-1} are associated with the 4f ($^2F_{5/2}$)–5d(^2E) transitions, whereas those at 44 700 and 50 310 cm^{-1} with the 4f ($^2F_{5/2}$)–5d (T_{2g}) transitions of Ce^{3+}. It is possible to identify the zero-phonon lines related to transitions to the two lowest-lying 5*d* levels, as well as some phonon replicas of these lines. The energies of the zero-phonon lines in the VIS-UV region as well as those of absorption lines in the infrared are listed in Table I, together with the identification of Ce^{3+} centers. The wide absorption bands peaked at 37 450 cm^{-1} and at 48 890 cm^{-1} in the YAG:Ce film are caused by the $^1S_0$-$^3P_1$ and $^1S_0$-$^1P_1$ transitions of the Pb^{2+} flux related impurity (so called A and B bands, respectively).[21,26]

Only one 0-phonon line is observed at lower energy side of each of the 4*f*-5*d* Ce^{3+} absorption bands. This confirms that they are associated with only one dominating Ce^{3+} site

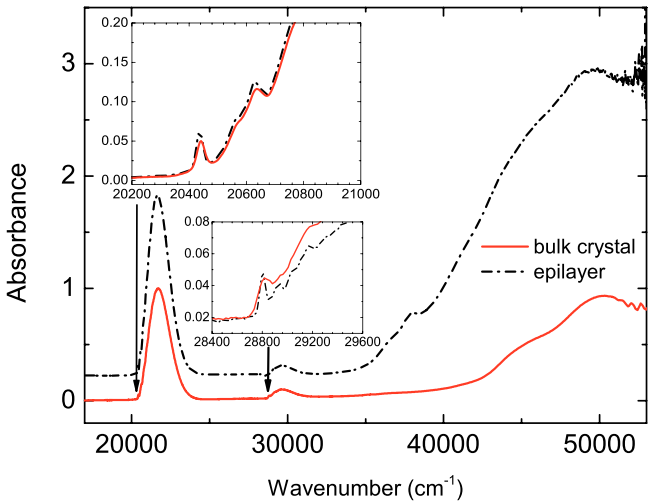

FIG. 4. Absorption spectra of YAG:Ce crystal and epitaxial layer at 15 K. Insets show expanded spectra around the 0-phonon lines.

($Ce^{3+}{}_Y$) in dodecahedral positions in YAG host. The $4f \rightarrow 5d$ transition bands for octahedral symmetry must be located at different energies than for dodecahedral sites (which is similar to cubic symmetry). Therefore, it is another confirmation that the second set of lines observed in the infrared region in bulk crystal is due to Ce^{3+} ions in the antisite octahedral positions ($Ce^{3+}{}_{Al}$). Energies of the absorption lines in the infrared and zero-phonon lines in the VIS-UV regions are listed in Table I for both types of Ce^{3+} centers.

The calculation of the energies of the Ce^{3+} $4f$ and $5d$ levels and CF parameters (CFP) for dodecahedral site with D_2 symmetry in YAG were performed in the framework of the exchange charge model (ECM).[22] Details of the calculation procedure can be found in Ref. 17. Using the standard notation of Wybourne[23] and Table 1.7 of Ref. 24, the parameterized effective Hamiltonians for the $4f^1$ and $5d^1$ configurations of Ce^{3+} ions in YAG can be, respectively, written as

$$\begin{aligned}\mathbf{H}(4f^1) = {} & E_{avg} + \zeta_{4f}\mathbf{s}_f \cdot \mathbf{l}_f + B_0^2(f)\mathbf{C}_0^{(2)} + B_2^2(f)(\mathbf{C}_2^{(2)} + \mathbf{C}_{-2}^{(2)}) \\ & + B_0^4(f)\mathbf{C}_0^{(4)} + B_2^4(f)(\mathbf{C}_2^{(4)} + \mathbf{C}_{-2}^{(4)}) \\ & + B_4^4(f)(\mathbf{C}_4^{(4)} + \mathbf{C}_{-4}^{(4)}) + B_0^6(f)\mathbf{C}_0^{(6)} \\ & + B_2^6(f)(\mathbf{C}_2^{(6)} + \mathbf{C}_{-2}^{(6)}) + B_4^6(f)(\mathbf{C}_4^{(6)} + \mathbf{C}_{-4}^{(6)}) \qquad (1)\end{aligned}$$

and

$$\begin{aligned}\mathbf{H}(5d^1) = {} & \Delta_E(fd) + \zeta_{5d}\mathbf{s}_d \cdot \mathbf{l}_d + B_0^2(d)\mathbf{C}_0^{(2)} + B_2^2(d) \\ & \times (\mathbf{C}_2^{(2)} + \mathbf{C}_{-2}^{(2)}) + B_0^4(d)\mathbf{C}_0^{(4)} + B_2^4(d) \\ & \times (\mathbf{C}_2^{(4)} + \mathbf{C}_{-2}^{(4)}) + B_4^4(d)(\mathbf{C}_4^{(4)} + \mathbf{C}_{-4}^{(4)}), \qquad (2)\end{aligned}$$

where the notation and meanings of various operators and parameters are defined according to the standard practice.[25,26] The resulting energies of the $4f$ and $5d$ levels of Ce^{3+} in dodecahedral sites in YAG are also listed in Table I, the appropriate parameters of the theoretical fit to the experimental data are given in Table II.

An excellent agreement between experimentally observed energies and theoretical calculations has been achieved for dominating $Ce^{3+}{}_Y$ center. Similar calculations for octahedral $Ce^{3+}{}_{Al}$ center are under way and will be reported in the forthcoming publication.

In conclusion, low temperature infrared absorption of YAG:Ce^{3+} bulk crystals grown by the Czochralski method shows evidence of multicenter incorporation of this dopant in bulk garnets. At least two major types of Ce^{3+} centers are observed. In epitaxially grown layers, only one set of lines is observed. Their energies are coincident with the energies of

TABLE I. Calculated and measured 4f and 5d CF energy levels of Ce^{3+} ions doped in YAG (data given in cm^{-1}). All CF energy states have the same Γ_5 representations in D_2 symmetry. The symbol "I.R." stands for the double-value irreducible representation of the parent group of D_2 (i.e., D_{2d} point-group). E_{calc} and E_{exp} correspond to the calculated and observed CF energy level values, respectively. The value in the bracket stands for the maximum of the measured 4f-5d absorption band. The maximums of the last two high-energy 4f-5d absorption bands were obtained by the Gaussian-shape decomposition.

			Bulk		LPE layer	Center
Level no.	^2L_J	I.R.	E_{calc}	E_{exp}	E_{exp}	designation
1	$^2F_{5/2}$	Γ_6	0	0	0	Ce_Y, Ce_{Al}
2		Γ_7	273	289	287	Ce_Y, Ce_{Al}
3		Γ_7	786			Ce_Y,
4	$^2F_{7/2}$	Γ_6	2097	2112	2013	Ce_Y
				2095		Ce_{Al}
5		Γ_6	2343	2342	2343	Ce_Y
				2330		Ce_{Al}
6		Γ_7	2458	2466	…[a]	Ce_Y
				2411	…[a]	Ce_{Al}
7		Γ_7	3822	3830	3830	Ce_Y
					3878	Ce_{Al}
8	$^2D_{3/2,5/2}$	Γ_7	20 442	20 442 (21 670)	20 433 (21 670)	Ce_Y
9		Γ_6	28 794	28 794 (29 710)	28 802 (29 710)	Ce_Y
10		Γ_6	43 472	(44 700)	(44 700)	Ce_Y
11		Γ_7	49 082	(50 310)	(50 310)	Ce_Y
12		Γ_7	60 534			Ce_Y

[a]These lines have too low intensity to be observed in epitaxial layers.

TABLE II. The energy parameters of Ce^{3+} ions doped in YAG in the framework of ECM (unit: all in cm^{-1} except the two G and α parameters). Details are given in Ref. 17. The abbreviations "*pc*," "*ec*," and "*corr*" stand for the CFP contributions from point charges, exchange charges, and the correction due to other factors, such as dipoles, respectively, and then "total" represents their sum.

	YAG							
	4f				5d			
	Pc	ec	corr	total	Pc	ec	corr	total
B_0^2	−318	131	731	544	−3382	16 032	7613	20 263
B_2^2	68	26	−156	−62	725	5228	−1632	4321
B_0^4	−321	159		−162	−4525	−2342		−6867
B_2^4	1642	1056		2698	23 157	24 241		47 398
B_4^4	−890	−738		−1628	−12 555	−10 295		−22 850
B_0^6	−937	−858		−1795				
B_2^6	326	328		654				
B_4^6	334	408		742				
B_6^6	304	457		761				
E_{avg}		1682				1682		
ΔE(fd)						38 783		
ξ		605				1082[a]		

[a]Reference 27.

the respective dominant lines in the bulk crystals. This testifies that the additional set of Ce^{3+} lines in YAG bulk crystals is associated with Ce^{3+} ions in octahedral (antisite) positions. Such antisites do not occur in epitaxial layers due to the low growth temperature. In contrast, they are expected to be formed during the high-temperature Czochralski growth. The layers exhibit very good optical quality, especially proved by much lower full-width at half of maximum of the Ce^{3+} lines associated with the $4f \rightarrow 4f$ transition than observed in bulk crystals. On the other hand, flux components used for LPE growth introduce unintentional impurities, as observed in the UV absorption spectrum of the epilayer. The theoretical crystal field calculations based on exchange-charge model describe very well the experimental data for the major $Ce^{3+}{}_Y$ center.

The cooperation program between Estonian and Polish Academies of Sciences for the years 2013–2015 is kindly acknowledged. This work was partially supported by the European Union within the European Regional Development Fund through the Innovative Economy grant MIME (POIG.01.01.02-00-108/09) and by the Polish National Science Center grant No. 2012/07/B/ST5/02376. C.G.M. and M.G.B. acknowledge support from (i) European Social Fund Grant GLOFY054MJD, (ii) European Social Fund's Doctoral Studies and Internationalisation Programme DoRa, and (iii) European Union through the European Regional Development Fund (Center of Excellence "Mesosystems: Theory and Applications," TK114).

[1]S. Kück, Appl. Phys. B: Lasers Opt. **72**, 515 (2001).
[2]A. A. Kaminskii, Laser Photonics Rev. **1**, 93 (2007).
[3]J. M. Robertson, M. W. Van Tol, W. H. Smits, and J. P. H. Heynen, Philips J. Res. **36**, 15 (1981).
[4]B. Hüttl, U. Troppenz, K. O. Velthaus, C. R. Ronda, and R. H. Mauch, J. Appl. Phys. **78**, 7282 (1995).
[5]E. Danielson, M. Devenney, D. M. Giaquinta, J. H. Golden, R. C. Haushalter, E. W. McFarland, D. M. Poojary, C. M. Reaves, W. H. Weinberg, and X. D. Wu, Science **279**, 837 (1998).
[6]J. L. Wu, G. Gundiah, and A. K. Cheetham, Chem. Phys. Lett. **441**, 250 (2007).
[7]J.-G. Kang, M.-K. Kim, and K.-B. Kim, Mater. Res. Bull. **43**, 1982 (2008).
[8]Y.-P. Fu, S.-B. Wen, and C.-S. Hsu, J. Alloys Compd. **458**, 318 (2008).
[9]M. Balcerzyk, Z. Gontarz, M. Moszynski, and K. Kapusta, J. Lumin. **87–89**, 963 (2000).
[10]M. Nikl, Meas. Sci. Technol. **17**, R37 (2006).
[11]A. Kamińska, A. Duzynska, M. Berkowski, S. Trushkin, and A. Suchocki, Phys. Rev. B **85**, 155111 (2012), and reference therein.
[12]C. R. Stanek, K. J. McClellan, M. R. Levy, C. Milanese, and R. W. Grimes, Nucl. Instrum. Methods Phys. Res. A **579**, 27 (2007).
[13]W. Nie, G. Boulon, and A. Montail, Chem. Phys. Lett. **164**, 106 (1989).
[14]Yu. Zorenko, V. Gorbenko, I. Konstankevych, A. Voloshinovskii, G. Stryganyuk, V. Mikhailin, V. Kolobanov, and D. Spassky, J. Lumin. **114**, 85 (2005).
[15]S. P. Feofilov, A. B. Kulinkin, T. Gacoin, G. Mialon, G. Dantelle, R. S. Meltzer, and C. Dujardin, J. Lumin. **132**, 3082 (2012).
[16]Yu. Zorenko, A. Voloshinovskii, V. Savchyn, T. Voznyak, M. Nikl, K. Nejezchleb, V. Mikhailin, V. Kolobanov, and D. Spassky, Phys. State Solidi B **244**, 2180 (2007).
[17]H. Przybylińska, C.-G. Ma, M. G. Brik, A. Kamińska, J. Szczepkowski, P. Sybilski, A. Wittlin, M. Berkowski, W. Jastrzębski, and A. Suchocki, Phys. Rev. B **87**, 045114 (2013).
[18]G. H. Dieke, *Spectra and Energy Levels of Rare Earth Ions in Crystals* (Interscience Publishers, New York, 1968).
[19]Yu. V. Zorenko, M. M. Batenchuk, V. I. Gorbenko, M. V. Pashkovskii, and I. V. Konstankevich. J. Appl. Spectrosc. **66**, 953 (1999).
[20]Yu. Zorenko, V. Gorbenko, I. Konstankevych, B. Grinev, and M. Globus, Nucl. Instrum. Methods Phys. Res. A **486**, 309 (2002).
[21]Yu. Zorenko, V. Gorbenko, T. Voznyak, and T. Zorenko, Phys. Status Solidi B **245**, 1618 (2008).
[22]B. Z. Malkin, in *Spectroscopy of Solids Containing Rare Earth Ions*, edited by A. A. Kaplyanskii and R. M. Macfarlane (North-Holland Publishing Company (Elsevier), Amsterdam, 1987), p. 13.
[23]B. G. Wybourne, *Spectroscopic Properties of Rare Earths* (Interscience Publishers, New York, 1965).
[24]G. K. Liu, in *Spectroscopic Properties of Rare Earths in Optical Materials*, edited by G. K. Liu and B. Jacquier (Tsinghua University Press, Heidelberg, 2005).
[25]W. T. Carnall, G. L. Goodman, K. Rajnak, and R. S. Rana, J. Chem. Phys. **90**, 3443 (1989).
[26]M. F. Reid, L. van Pieterson, R. T. Wegh, and A. Meijerink, Phys. Rev. B **62**, 14744 (2000).
[27]M. F. Reid, L. van Pieterson, and A. Meijerink, J. Alloys Compd. **344**, 240 (2002).